Buffer-gas-induced shift and broadening of hyperfine resonances in alkali-metal vapors

P. J. Oreto, Y.-Y. Jau, A. B. Post, N. N. Kuzma, and W. Happer
Department of Physics, Princeton University, Princeton, New Jersey 08544, USA
(Received 5 December 2003; published 20 April 2004)

We review the shift and broadening of hyperfine resonance lines of alkali-metal atoms in buffer gases. We present a simple theory both for the shift and the broadening induced by He gas. The theory is parametrized by the scattering length of slow electrons on He atoms and by the measured hyperfine intervals and binding energies of the *S* states of alkali-metal atoms. The calculated shifts and their temperature dependence are in good agreement with the published experimental data. The calculated broadening is 1.6 times smaller than the recent measurements, and more than 20 times smaller than the earlier measurements. We attribute much of the linewidth in the earlier experiments to possible small temperature gradients and the resulting inhomogeneous line broadening from the temperature dependence of hyperfine frequency shift at constant buffer-gas pressure.

DOI: 10.1103/PhysRevA.69.042716 PACS number(s): 34.30.+h, 06.30.Ft, 32.10.Fn, 95.30.Ky

I. INTRODUCTION

The magnetic-resonance frequencies of optically pumped alkali-metal atoms in buffer-gas cells have long been used in compact, portable frequency standards [1] and magnetometers [2]. The buffer gas is needed to slow down the diffusion of optically pumped atoms to the cell walls, which tend to depolarize the atoms. The buffer gas broadens the linewidth and shifts the frequency of the microwave resonance by an amount that depends on temperature and is proportional to buffer-gas pressure. Higher buffer-gas pressures will be needed to mitigate the faster diffusional losses of polarized atoms to the cell walls in proposed miniaturized atomic clocks [3,4]. Thus there is renewed interest in the frequency shift and line broadening induced by the buffer gases. The shifts measured in different laboratories are in fairly good agreement with each other [5–8]. However, there appear to be only two experiments [9,10] from which microwave resonance linewidths can be inferred. These results differ from each other by more than a factor of 10. It would be thus useful to understand this large discrepancy.

In this paper we consider alkali-metal atoms in helium gas, a system for which simple and fairly reliable theoretical estimates of the pressure shifts and damping rates are possible. The estimates obtained in this work are in good agreement with previous measurements of the frequency shifts and their temperature dependence. The homogeneous line broadening recently measured by Walter *et al.* [9] is about 1.6 times larger than the theoretical predictions of this paper, but the earlier measurements of Vanier *et al.* [10] imply a linewidth that is more than 20 times larger. As we discuss below, it appears that much of the linewidth in the earlier experiments was due to small temperature gradients [11] and the resulting inhomogeneous line broadening from the temperature dependence of the frequency shift.

For optically pumped alkali-metal atoms in He gas, most of the physics is captured by the Fermi pseudopotential [12]

$$V_F(\mathbf{r},\mathbf{R}) = \frac{2\pi\hbar^2 a}{m_e}\delta(\mathbf{r}-\mathbf{R}), \tag{1}$$

where $\mathbf{r}$ and $\mathbf{R}$ are the displacements of the alkali valence electron and the He nucleus, respectively, from the nucleus of the alkali-metal atom. The electron mass is m_e, and the scattering length for slow electrons on He atoms [13] is $a = 0.63$ Å. The simple potential (1) was first introduced by Fermi [12] to account for the pressure shifts of optical absorption lines in alkali-metal vapors. The interactions between alkali-metal atoms and heavier, more polarizable buffer gases (for example, Ar atoms or N_2 molecules) have non-negligible long-range interactions that cannot be described by the Fermi pseudopotential alone. Thus we will consider only He in this work.

II. BORN-OPPENHEIMER POTENTIALS

The Born-Oppenheimer potential $V=V(R)$ is the energy required to bring an alkali-metal atom and a buffer-gas atom from infinite separation to a separation R. Potentials V can be found that are consistent with the cross sections of alkali-metal atom scattering from buffer-gas atoms, notably from the noble-gas atoms [14]. However, these experimentally based potentials are not unique, and they do not seem to be available for He gas.

We denote the unperturbed wave function of the valence electron in the alkali-metal atom by $\phi_{gljm}(\mathbf{r},\sigma)$. The electron-spin variable is $\sigma=\pm 1/2$. The ground-state principal quantum numbers g are 3, 4, 5, and 6 for Na, K, Rb, and Cs atoms, respectively. The orbital, total, and azimuthal angular-momentum quantum numbers are $l=0$, $j=1/2$, and $m=\pm 1/2$. We take the Born-Oppenheimer potential to be the expectation value of the Fermi potential as follows:

$$V(R) = \int d^3\mathbf{r}|\phi_{gljm}(\mathbf{r},m)|^2 V_F(\mathbf{r},\mathbf{R}) = \frac{\hbar^2 a P_{g0}^2(R)}{2m_e R^2}. \tag{2}$$

We assume valence-electron wave functions of the form

$$\phi_{nljm}(\mathbf{r},\sigma) = \frac{P_{nl}}{r}\sum_{m_l m_s} Y_{lm_l}\chi_{m_s} C^{jm}_{l,m_l,1/2,m_s}. \tag{3}$$

Here $P_{nl}=P_{nl}(r)$ is the radial wave function, the spherical harmonic $Y_{lm_l}=Y_{lm_l}(\theta,\phi)$ is a function of the colatitude angle θ and azimuthal angle ϕ of $\mathbf{r}$, the spin basis function is

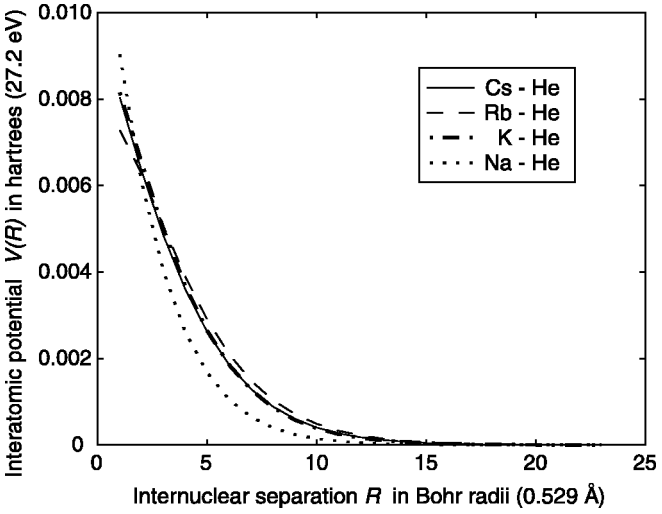

FIG. 1. Theoretical Born-Oppenheimer potentials $V(R)$ for alkali-metal atoms interacting with He atoms, calculated from Eq. (2).

$\chi_{m_s}=\chi_{m_s}(\sigma)=\delta_{\sigma m_s}$, and $C^{jm}_{l,m_l,1/2,m_s}$ is a Clebsch-Gordan coefficient [15]. We will use atomic units, with distances r measured in Bohr radii ($a_B=5.29\times10^{-9}$ cm), and energies E_{nlj} measured in hartrees (27.2 eV).

We have evaluated Eq. (2), and the results are plotted in Fig. 1. For Na, K, and Rb we used the conveniently tabulated Hartree-Fock wave functions of Clementi and Roetti [16]. The tables of Clementi and Roetti include atoms with $Z\leqslant54$. For Cs with $Z=55$ we used the Coulomb wave functions, discussed in connection with Eq. (11) below. The Coulomb wave functions differ only by a few percent from the Clementi-Roetti wave functions for the values $r\geqslant4$ of interest for this work. The potentials of Eq. (2) are nearly the same as those estimated by Pascale [17].

III. MODIFICATION OF THE HYPERFINE COUPLING

The He atom will perturb the ground-state wave function of the valence electron of the alkali-metal atom. We write the perturbed wave function as

$$\psi_{gljm}(\mathbf{r},\mathbf{R},\sigma)=\phi_{gljm}(\mathbf{r},\sigma)+\delta\phi_{gljm}(\mathbf{r},\mathbf{R},\sigma). \tag{4}$$

We assume that we can use the Fermi potential of Eq. (1) and the first-order perturbation theory to write

$$\delta\phi_{gljm}(\mathbf{r},\mathbf{R},\sigma)=\frac{2\pi\hbar^2a}{m_e}\sum\frac{\phi_{nl'j'm'}(\mathbf{r})\phi^*_{nl'j'm'}(\mathbf{R},\sigma)\phi_{gljm}(\mathbf{R},\sigma)}{E_{glj}-E_{nl'j'}}. \tag{5}$$

The sum extends over all excited states $\phi_{nl'j'm'}(\mathbf{r},\sigma)$ of the valence electron. The unperturbed energies of the excited states are $E_{nl'j'}$ and the unperturbed energy of the ground state is E_{glj}.

The scalar magnetic-dipole coupling $A\mathbf{I}\cdot\mathbf{S}$ of the nuclear spin $\mathbf{I}$ of a ground-state alkali-metal atom to the electron spin $\mathbf{S}$ has a coupling coefficient [18]

$$A=\frac{8\pi g_S\mu_B\mu_I}{3I}|\psi_{gljm}(0,\mathbf{R},m)|^2. \tag{6}$$

Here I is the nuclear-spin quantum number, the Bohr magneton is $\mu_B=9.274\times10^{-21}$ erg G^{-1}, the g factor of the electron is $g_S=2.0023$, and the magnetic moment of the alkali nucleus is μ_I. By symmetry, the coupling coefficient $A=A(R)$ depends on the magnitude, but not on the direction of $\mathbf{R}$. According to Eq. (4), the spherical symmetry of the valence-electron wave function is perturbed by the buffer-gas atom, so an anisotropic magnetic-dipole hyperfine interaction and an electric quadrupole interaction with the nucleus will be induced. These anisotropic hyperfine interactions will produce zero-frequency shift after averaging over all orientations, and the numerical estimates by Walter *et al.* [19] show that they are not large enough to appreciably affect the spin relaxation (line broadening), so we will ignore them.

The magnetic-dipole coupling coefficient (6) can be written as

$$A=A_g+\delta A_g, \tag{7}$$

where the coupling coefficient for a free atom in an S state with $l=0$ is

$$A_n=\frac{8\pi g_S\mu_B\mu_I}{3I}\phi^2_{nljm}(0,m). \tag{8}$$

We assume that $\phi_{nljm}(0,m)$ is a real number.

To first order in $\delta\phi_{gljm}(0,\mathbf{R},m)$, the shift of the ground-state coupling coefficient (6) is

$$\delta A_g=\frac{16\pi g_S\mu_B\mu_I}{3I}\phi_{gljm}(0,m)\,\delta\phi_{gljm}(0,\mathbf{R},m). \tag{9}$$

Combining Eqs. (9) and (6), we find that the collisionally induced shift of the hyperfine coupling coefficient is

$$\frac{\delta A_g}{A_g}=\frac{\hbar^2a}{m_eR^2}\sum_{n>g}\sqrt{\frac{A_n}{A_g}}\frac{P_{n0}(R)P_{g0}(R)}{E_{glj}-E_{nlj}}. \tag{10}$$

The sum extends over all excited S states ($l=0$ and $j=1/2$) with $n>g$.

For the ground-state wave functions of Na, K, and Rb we used the tabulated values of Clementi and Roetti [16]. For the ground state of Cs and for the excited S states of all alkali-metal atoms, we used Coulomb-approximation wave functions [20]:

$$P_{n0}=\sum_{q=0}^{p}c_qe^{-r/n^*}r^{n^*-q}, \tag{11}$$

where the effective quantum number n^* is written as

$$n^*=\frac{1}{\sqrt{2(E_\infty-E_{nlj})}}, \tag{12}$$

with E_∞ denoting the ionization energy of the atom. The coefficients c_q of the sum can be calculated starting from c_0, using the recurrence formula

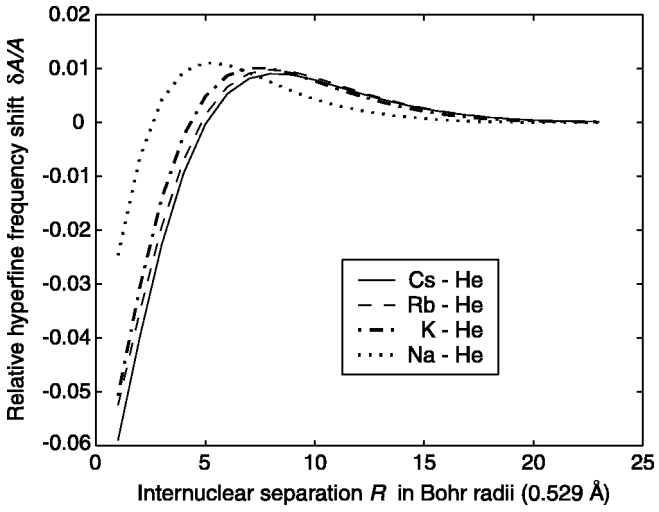

FIG. 2. Relative shift in hyperfine frequency, induced by helium gas on alkali-metal atoms, calculated from Eq. (10).

$$c_q = -\frac{n^*(n^*-q)(n^*-q+1)}{2q}c_{q-1}. \tag{13}$$

The upper limit p of the asymptotic series of Eq. (11) was chosen to get the best convergence for $r=1$, slightly inside the core of the atom. The wave functions were normalized such that $\int_1^\infty P_{n0}^2 dr = 1$. The small probability to find the electron at $r<1$ was negligible, even for the ground state. For temperatures on the order of 100 °C, the thermal energy is so small compared to the repulsive Born-Oppenheimer potential that helium and alkali-metal atoms almost never get closer to each other than $r=4$. The binding energies E_{nlj} needed in Eq. (12) were taken from the experimental data tabulated by Moore [21], and the hyperfine coupling coefficients A_n are experimental values taken from the review article of Arimondo *et al.* [22]. The sum in Eq. (10) was extended to $n=\infty$ by assuming that the binding energies $E_\infty - E_{nlj}$, the hyperfine interaction coefficients A_n, and the radial wave functions $P_{n0}(R)$ scale as power laws in n, which is expected and is also observed from the experimental data [21,22].

We have evaluated Eq. (10), the relative shift in resonance frequency as a function of R, for the alkali-metal atoms Na through Cs, and sketched the results in Fig. 2.

IV. EVOLUTION OF THE DENSITY MATRIX

It is convenient [9] to discuss the properties of existing isotopes of alkali-metal atoms in terms of a hypothetical isotope with nuclear-spin quantum number $\bar{I}=1/2$ and nuclear magnetic moment $\mu_{\bar{I}}=\mu_N=eh/2m_pc$. From Eq. (6), we see that the ratio of the hyperfine coupling coefficient A_n of an existing isotope with magnetic moment μ_I and nuclear-spin quantum number I to the coupling coefficient $\bar{A}_n$ of the hypothetical isotope is

$$\eta_I = A_n/\bar{A}_n = \frac{\mu_I}{2I\mu_N}. \tag{14}$$

At the center of a ground-state alkali-metal atom, the valence-electron spin produces a magnetic field of magnitude $B=\bar{A}_g/4\mu_N=0.121$, 0.393, 0.581, 1.22, and 2.05 MG for Li, Na, K, Rb, and Cs, respectively. Numerical values of $\bar{A}_g/h$ for the ground states of the alkali-metal atoms are summarized in Table I.

TABLE I. Hyperfine coupling coefficients $\bar{A}_g/h$ for hypothetical alkali-metal atoms with a nuclear-spin quantum number $\bar{I}=1/2$, and with a nuclear moment of one nuclear magneton. The small hyperfine-structure anomalies, less than 1% for the heaviest atoms, have been ignored.

Atom	Li	Na	K	Rb	Cs
Ground state	2^2S	3^2S	4^2S	5^2S	6^2S
$\bar{A}_g/h$ (GHz)	0.370	1.198	1.772	3.734	6.238

The pressure shift is caused by the interaction

$$V_{\rm ps} = \delta A_g \mathbf{I}\cdot\mathbf{S}, \tag{15}$$

which acts during binary collisions between helium and alkali-metal atoms. The density matrix ρ of the alkali-metal atoms will evolve due to interaction (15) at the rate

$$\dot{\rho} = \frac{\langle \delta A_g\rangle}{i\hbar}[\mathbf{I}\cdot\mathbf{S},\rho] + \frac{\eta_I^2\Gamma_{\rm C}}{2}(2\{\mathbf{I}\cdot\mathbf{S}\}\rho\{\mathbf{I}\cdot\mathbf{S}\} - \{\mathbf{I}\cdot\mathbf{S}\}^2\rho - \rho\{\mathbf{I}\cdot\mathbf{S}\}^2). \tag{16}$$

Here the collision-induced change δA_g in the coupling coefficient for an existing isotope will be related to that of the hypothetical isotope by $\delta A_g = \eta_I \delta\bar{A}_g$.

From Eq. (16) we see that the rate of change of the density matrix is parametrized by the mean shift $\langle \delta A_g\rangle$ of the hyperfine coupling coefficient and by the Carver rate $\Gamma_{\rm C}$ [9]. We discuss both parameters in more detail below.

V. THEORETICAL PRESSURE SHIFT

For alkali-metal atoms at relatively low magnetic fields (like those of atomic clocks), the energy-basis states $|fm\rangle$ are well described by a total angular-momentum quantum number $f=a=I+1/2$ or $f=b=I-1/2$ and by an azimuthal quantum number m. The basis states are very nearly eigenstates of $\mathbf{I}\cdot\mathbf{S}$ with $2\mathbf{I}\cdot\mathbf{S}|am\rangle = I|am\rangle$ and $2\mathbf{I}\cdot\mathbf{S}|bm\rangle = -(I+1)|am\rangle$.

If we take the matrix elements of Eq. (16) between the initial state $|a,m_a\rangle$ and $|b,m_b\rangle$ of a typical clock transition, we find

$$\langle am_a|\dot{\rho}|bm_b\rangle = (-i\delta\omega - \gamma)\langle am_a|\rho|bm_b\rangle + \cdots, \tag{17}$$

where γ is defined in the beginning of Sec. VI below and "…" denotes coupling to other components of the density matrix. The frequency shift is

$$\delta\omega = \frac{[I]\langle \delta A_g\rangle}{2\hbar} = Na_B^3\omega_0\lambda, \tag{18}$$

where $[I]$ denotes $2I+1$, N is the number density of He atoms, and $\omega_0=[I]A_g/2\hbar$ is the unperturbed frequency of the clock transition. The dimensionless, isotope-independent parameter λ was introduced by Bean and Lambert [8]. Experi-

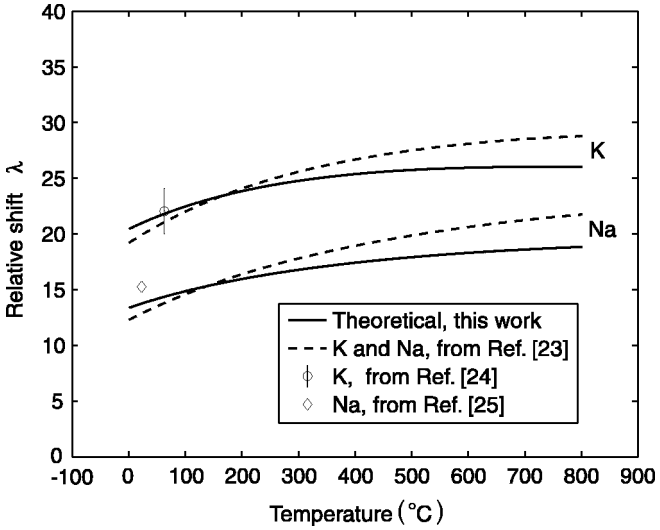

FIG. 3. Relative shifts λ for Na and K atoms, induced by helium gas. The solid lines are obtained theoretically from Eq. (19). The dashed lines are the temperature-dependent measurements of Bean and Lambert [23]. Additional experimental data points are from Bloom and Carr [24] for K, and from Ramsey and Anderson [25] for Na.

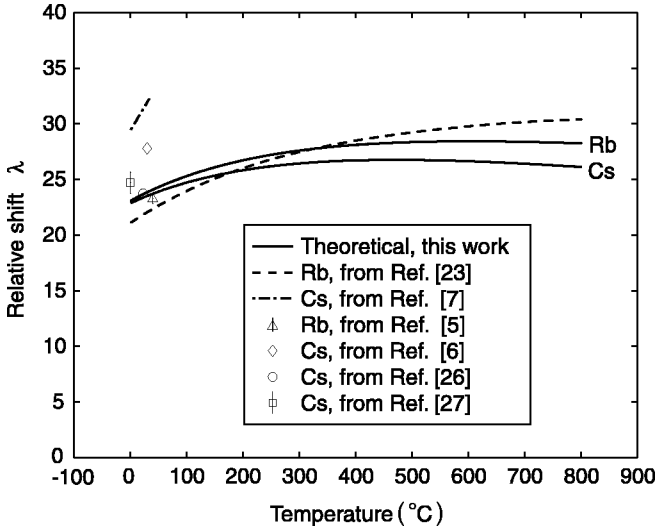

FIG. 4. Relative shifts for Rb and Cs atoms, induced by helium gas. The solid lines are obtained theoretically from Eq. (19). The temperature-dependent measurements are shown with the dashed line for Rb (Bean and Lambert [23]) and with the dash-dotted line for Cs (Arditi and Carver [7]). Additional experimental data points are from Ref. [5] for Rb and from Refs. [6,26,27] for Cs, as indicated in the legend.

mentally, $\lambda = \delta\omega/\omega_0 N a_B^3$ is determined in accordance with Eq. (18) from measured values of the frequency shift $\delta\omega$ in a gas of number density N. Bean and Lambert [8] show that λ can be obtained theoretically from the statistical average

$$\lambda = \frac{1}{a_B^3}\int_0^\infty \frac{\delta A_g}{A_g} e^{-V/kT} 4\pi R^2 dR, \tag{19}$$

where $k = 1.38 \times 10^{-16}$ erg K^{-1} is the Boltzmann constant and T is the absolute temperature. The results of evaluating Eq. (19) with the values of V from Eq. (2) and δA_g from Eq. (10) are shown in Figs. 3 and 4, together with the experimental data evaluated according to Eq. (18). The theory is in reasonably good agreement with the systematic experimental measurements of λ by Bean and Lambert [23] for Na, K, and Rb, and in fair agreement with other experimental determinations of λ.

VI. THEORETICAL CARVER RATE

The damping rate from Eq. (17) is

$$\gamma = \frac{\eta_I^2 [I]^2 \Gamma_C}{8}. \tag{20}$$

We assume that the orbit of the colliding pair is a classical path, defined by the Born-Oppenheimer potential (2), the impact parameter b, and the initial relative velocity v at infinite separation $R = \infty$, where $V(R) = 0$. For problems of this type, it is known that classical-path theories give the same answer as partial-wave theories to 1% or better [28]. The radial speed $u = u(R) = |dR/dt|$ at the separation R is

$$u = v\sqrt{1 - \frac{b^2}{R^2} - \frac{2V}{Mv^2}}, \tag{21}$$

where M is the reduced mass of the pair. We choose the origin of time such that the closest approach distance $s = s(b,v)$, defined by $u(s) = 0$, is attained at $t = 0$. In a classical-path approach the Carver rate [9] is given by

$$\Gamma_C = N\int_0^\infty dv w v \int_0^\infty db 2\pi b \phi^2. \tag{22}$$

Here the phase $\phi = \phi(b,v)$, accumulated as the result of a collision between an alkali-metal atom and a buffer-gas atom, is

$$\phi = \int_{-\infty}^{\infty} \frac{dt}{\hbar}\overline{\delta A_g} = 2\int_s^\infty \frac{dR}{\hbar u}\overline{\delta A_g}. \tag{23}$$

The initial relative speed v of the colliding pair has the Maxwell distribution, $w = w(v,T)$,

$$w = 4\pi v^2 \left(\frac{M}{2\pi kT}\right)^{3/2} e^{-Mv^2/2kT}. \tag{24}$$

The temperature dependence of the Carver rate at constant helium density is given by

$$\Gamma_C' = \frac{\partial \Gamma_C}{\partial T} = N\int_0^\infty dv \frac{\partial w}{\partial T} v \int_0^\infty db 2\pi b \phi^2, \tag{25}$$

where from Eq. (24) we find

TABLE II. Calculated Carver rates $\Gamma_C/[\mathrm{He}]$ and their temperature coefficients $\Gamma'_C/[\mathrm{He}]$, where [He] is the helium gas density in amagats. The values were calculated for a temperature $T=100\,^\circ$C with the Born-Oppenheimer potentials $V(R)$ of Fig. 1 and with the hyperfine coupling perturbations $\delta\bar{A}_g$ that follow from Fig. 2.

	^{3}He		^{4}He	
Alkali metal	$\Gamma_C/[\mathrm{He}]$ (s^{-1} amagat^{-1})	$\Gamma'_C/[\mathrm{He}]$ (s^{-1} amagat^{-1} K^{-1})	$\Gamma_C/[\mathrm{He}]$ (s^{-1} amagat^{-1})	$\Gamma'_C/[\mathrm{He}]$ (s^{-1} amagat^{-1} K^{-1})
Na	6.20	0.0043	7.12	0.0048
K	23.6	0.012	26.5	0.014
Rb	123.3	0.051	139.5	0.056
Cs	334.1	0.065	377.3	0.073

$$\frac{\partial w}{\partial T}=\frac{w}{T}\left(\frac{Mv^2}{2kT}-\frac{3}{2}\right). \tag{26}$$

Numerical values of Γ_C and Γ'_C, calculated from Eqs. (22) and (25), are summarized in Table II. The helium density in amagats is

$$[\mathrm{He}]=\frac{N}{N_L}, \tag{27}$$

where the Loschmidt constant $N_L=2.6868\times10^{19}$ cm^{-3} is defined as the number density of an ideal gas at a pressure $p=760$ torr (1 atm) and temperature $T=273.15$ K (0 °C).

VII. CARVER RATE MEASUREMENTS

We know of only two direct or implicit Carver rate measurements: the pioneering study by Vanier *et al.* [10] of ^{85}Rb relaxation in ^{4}He, from which Carver rates can be inferred, and more recent direct measurements of Carver rates of Rb in ^{3}He by Walter *et al.* [9]. Since the experimental results are so different from each other, and since the rates measured in Ref. [10] are so much larger than either our theoretical predictions or the measurements of Ref. [9], we will review both experimental procedures in some detail and comment on what we think the cause of the large discrepancy is.

Vanier *et al.* [10] made systematic measurements of the damping rates of ^{85}Rb in the gases ^{4}He, Ne, N_2, and Ar. A spherical quartz cell, with a radius $R_c\approx3.5$ cm, contained a buffer gas and a small amount of ^{85}Rb metal. The cell was centered in a TE_{011} cylindrical microwave cavity. A small static field, on the order of 1 G in magnitude, was directed along the axis of the cavity. Resonant light from a ^{85}Rb lamp passed through a ^{87}Rb filter cell that absorbed light that could have pumped ^{85}Rb atoms from the hyperfine multiplet with $f=a=3$. The filtered pumping light passed along the axis of the cavity into the cell and produced a population inversion, with more ^{85}Rb atoms in the high-energy multiplet with $f=a=3$ than in the low-energy multiplet with $f=b=2$. The light was unpolarized, so there should have been very nearly equal populations of sublevels with different azimuthal quantum numbers m but within the same multiplet f. Some slight inequalities of the populations with different values of $|m|$ (a small tensor polarization) could have been produced [29,30], but they would have had negligible effect on the experimental observations.

The atoms were optically pumped long enough to reach steady-state conditions. Then the pumping light was turned off, and a short time later a pulse of microwaves was transmitted to the cavity. The microwave frequency equaled that of the "0-0 resonance" between the sublevels $|fm\rangle=|30\rangle$ and $|fm\rangle=|20\rangle$. The magnetic moment of the atoms, coherently oscillating during the 0-0 transition, coupled some of their microwave power into the cavity, and part of this power emerged from the cavity via a transmission line, where it was monitored with a heterodyne detector. The amplitude of the free induction decay (FID) signal as a function of time t was fit to an envelope $e^{-\gamma_2 t}$, to extract the decay rate γ_2. By varying the He pressure p, it was determined that the dependence of the decay rate on pressure was well described by

$$\gamma_2=\frac{\pi^2}{R_c^2}D_0\frac{p_0}{p}+N\bar{v}\sigma_2+\gamma_2^{se}. \tag{28}$$

The first term describes the losses of coherently oscillating Rb atoms due to diffusion through the buffer gas to the cell walls. The diffusion coefficient at the reference pressure $p_0=760$ torr is D_0. The second term describes the homogeneous damping due to collisions of ^{85}Rb atoms with He atoms of number density N. The thermally averaged cross section is σ_2, and the mean relative velocity of a colliding He-Rb pair is $\bar{v}=\sqrt{8kT/\pi M}=1.29\times10^5$ cm s^{-1}, where the reduced mass of the pair is $M=3.82$ a.u. and $T=300.15$ K is the absolute temperature of the experiments (27 °C). The final term $\gamma_2^{se}=\gamma_2^{se}(T)$ describes the damping due to spin-exchange collisions between pairs of Rb atoms, which were assumed to have the density of a saturated vapor at the temperature T.

The homogeneous, collisional damping rate of the 0-0 coherence, described by the cross section σ_2, is a linear combination of two rates: (1) The Carver rate Γ_C due to the pressure shift interaction of Eq. (15); and (2) the S-damping rate Γ_{sd} due to the spin-rotation interaction $\gamma\mathbf{S}\cdot\mathbf{N}$ during Rb-He collisions [31,32].

In analogy to Eq. (16), the contribution of spin-rotation interactions to the evolution of the density matrix is $\dot{\rho}=\Gamma_{sd}(-3\rho/4+\mathbf{S}\cdot\rho\mathbf{S})$. Substituting $\rho=|a0\rangle\langle b0|$ into this ex-

pression, and evaluating the self-coupling term, we see that *S*-damping makes a contribution $\frac{3}{4}\Gamma_{sd}$ to γ_2. The contribution to γ_2 from the Carver rate is given by Eq. (20), so the measured value $\sigma_2 = 294 \times 10^{-24}$ cm^2 should be determined by

$$N\bar{v}\sigma_2 = \frac{3}{4}\Gamma_{sd} + \frac{\eta_I^2[I]^2\Gamma_C}{8}. \tag{29}$$

For ^{85}Rb, $I = \frac{5}{2}$, $\mu_I/\mu_N = 1.3527$, and $\eta_I = 0.2706$.

Vanier *et al.* also measured the initial amplitude of the FID as a function of the delay time t_d between the termination of the optical pumping and the application of the microwave pulse. They found that the initial amplitude decayed exponentially as $e^{-\gamma_1 t_d}$. They were able to fit their measured values γ_1 versus the gas pressure p to obtain an expression analogous to Eq. (28), and they deduced a longitudinal relaxation cross section σ_1, which is related to the *S*-damping rate Γ_{sd} by

$$\frac{\Gamma_{sd}}{[X]} = N_L\bar{v}\sigma_1. \tag{30}$$

Here the number density of the buffer gas X in amagats is $[X] = N/N_L$, in analogy to Eq. (27). Combining Eqs. (29) and (30), we find

$$\frac{\Gamma_C}{[X]} = \frac{8N_L\bar{v}}{\eta_I^2[I]^2}\left(\sigma_2 - \frac{3}{4}\sigma_1\right). \tag{31}$$

The values σ_1 were too small to measure for He or Ne.

Recently, Walter *et al.* have measured the dependence of the most slowly damping longitudinal mode of spin polarization for Rb atoms in He, N_2, and Ar buffer gases as a function of magnetic field, ranging from nearly zero to many thousands of gauss. The slowing down of this late-time relaxation rate as the magnetic field increases is called magnetic decoupling. The spin relaxation due to *S*-damping is slowed down by a factor $\langle S_z\rangle/\langle F_z\rangle$, the fraction of the total spin $\langle F_z\rangle = \langle S_z\rangle + \langle I_z\rangle$ that is carried by the electron. This slowing down of the relaxation is sometimes called the "nuclear flywheel" effect, since it is due to the replenishment of the electron-spin polarization destroyed in an *S*-damping collision (hence, the name "*S*-damping") by the hyperfine coupling to the still-polarized nuclear-spin [9] in the time between collisions. The magnetic decoupling curve has its minimum width when both the Carver rate and the spin-exchange rate are negligible compared to the *S*-damping rate. The spin-exchange rate is very temperature dependent, since the Rb number density in a saturated vapor increases rapidly with temperature. The *S*-damping rate coefficient also has a substantial temperature dependence [9,33]. The temperature dependence of the Carver rate was too small to measure in the work of Walter *et al.*, and as one can see from Table II, little experimental temperature dependence is predicted theoretically. By quantitatively analyzing the magnetic decoupling curves of ^{85}Rb and ^{87}Rb in cells with various gas pressures and at different temperatures, Walter *et al.* [9] were able to determine both the Carver rates and the *S*-damping rates for Rb in ^{3}He, N_2, and Ar gases.

TABLE III. A comparison of experimental values of the Carver rates Γ_C and the *S*-damping rates Γ_{sd} for Rb in the buffer gases He, Ne, N_2, and Ar at 27 °C. Theoretical predictions of Γ_C from Table II are also shown for Rb in ^{3}He and ^{4}He, the gases used by Refs. [9,10], respectively. The experimental values of Γ_{sd} rates of Ref. [9] have been extrapolated to 27 °C with the linear temperature dependencies quoted therein.

Gas,	$\Gamma_C/[X]$ (s^{-1} amagat^{-1})				$\Gamma_{sd}/[X]$ (s^{-1} amagat^{-1})	
X	Ref. [9]	Theory	Ref. [10]	Theory	Ref. [9]	Ref. [10]
He	191	120	3093	135	8.5	≈0
Ne			2828			≈0
N_2	395		3062		115	118
Ar	≈0		14		610	637

The experimental measurements of Carver rates and *S*-damping rates for Rb in various buffer gases as well as the theoretical predictions of the Carver rate for He are summarized in Table III. Neither measurement in helium gas is equal to the theoretical predictions, but the measurement of Ref. [9] is only a factor of 1.6 larger than theory. The theoretical prediction of the Carver rate in Eq. (22) involves the square of the theoretically estimated value of $\delta\bar{A}_g$, integrated over a classical path. This will magnify small discrepancies in $\delta\bar{A}_g$, compared to the shift calculation of Eq. (19), which involve only a Boltzmann statistical average over $\delta\bar{A}_g$. Given the good, but not perfect, agreement between the theoretical and the experimental values of the shift in Figs. 3 and 4, a discrepancy by a factor of 1.6 in the broadening is not unreasonable.

VIII. INHOMOGENEOUS BROADENING

Recent measurements [34] of the linewidths of Zeeman and microwave resonances of ^{87}Rb in N_2 are fully consistent with the linewidths predicted using the data of Ref. [9] and inconsistent with the data of Ref. [10]. From inspection of Table III we see that there is actually a very good agreement between the data of Refs. [9] and [10], except for the Carver rates Γ_C of He and N_2, where the results differ by about a factor of 10. Both experiments measure very small Carver rates for Ar. As we explain in this section, we think that the rates measured in Ref. [10] included inhomogeneous damping due to a small temperature spread $\Delta T < 1$ °C in the relatively large sample cells [11].

Bean and Lambert [23] have measured the microwave frequencies ν for ^{23}Na, ^{39}K, and ^{85}Rb in the buffer gases He, Ne, Ar, and N_2 for temperatures T ranging from about −125 °C to 800 °C. They summarize their measurements with a quantity

$$(\nu - \nu_0)/P = \beta. \tag{32}$$

The microwave frequency for free atoms with no buffer gas is ν_0, and P is defined as $P = p/p_{10}$, where $p_{10} = 10$ torr.

The parameter $\beta = \beta(T)$ depends only on temperature T and it is the shift of the ground-state hyperfine frequency at

the temperature T in a buffer gas with the number density N_B of an ideal gas at a pressure of 1 cm Hg (10 torr) and a temperature of 300 °C,

$$N_B = \frac{1}{76} N_L \frac{273.15}{300} = 3.2193 \times 10^{17}\ \mathrm{cm}^{-3}. \tag{33}$$

The hyperfine frequency ν for the alkali-metal isotope in a gas of number density N and temperature T is therefore

$$\nu = \nu(N,T) = \nu_0 + \beta \frac{N}{N_B}. \tag{34}$$

We assume that the buffer gases obey the ideal-gas law, so the gas pressure p is

$$p = NkT. \tag{35}$$

We can use Eqs. (34) and (35) to write ν as a function of p and T,

$$\nu = \nu(p,T) = \nu_0 + \frac{\beta p}{N_B kT}. \tag{36}$$

We note that the parameter β of Eq. (32), measured and tabulated in Ref. [23], is related to the dimensionless parameter λ of Eq. (19), measured and tabulated in Ref. [8], by

$$\lambda = \frac{\beta}{N_B a_B^3 \nu_0}. \tag{37}$$

The sealed-off cells used by Vanier *et al.* [10] were isobaric, but they may have had small temperature gradients, e.g., with the gas at the top of the cell slightly hotter than the gas at the bottom.

Using Eq. (36) and the data of Bean and Lambert [23], we have plotted in Fig. 5 the frequency shift versus temperature for cells with 1 atm of gas pressure. We have also indicated the inhomogeneous line broadening $\Delta\nu_p$ that would occur for a temperature spread of 20 °C. This is an unrealistically large gradient, chosen to illustrate the point, not to imply that gradients that large are suspected for the experiments of Ref. [10]. From Fig. 5 it is clear that Ar is about ten times less sensitive to the line broadening due to temperature gradients than are He, Ne, or N_2 gases.

To estimate how large the temperature gradient would have had to be to account for a substantial fraction of the damping observed by Vanier *et al.* [10], let us assume that the temperature in sealed-off cells can be written as

$$T = \overline{T} + \delta T, \tag{38}$$

where $\overline{T}$ is the mean temperature and $\delta T = \delta T(\mathbf{r}_c)$ is a small inhomogeneity that depends on the location $\mathbf{r}_c$ within the cell. The gas in the cell will be at a constant pressure p, so we can use Eq. (38) to show that the resonant frequency at the point $\mathbf{r}_c$ is

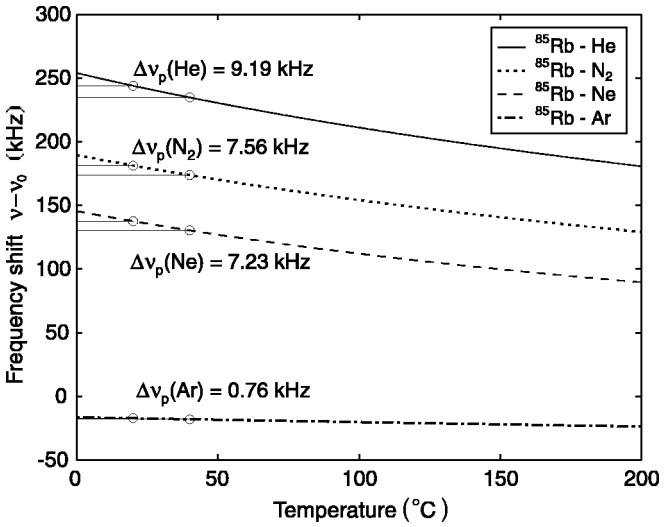

FIG. 5. Absolute hyperfine frequency shifts of ^{85}Rb induced by the buffer gases at a constant pressure $p=760$ torr, inferred from the data of Bean and Lambert [8]. Also shown are the spreads in frequency $\Delta\nu_p$ that would be caused by a spread in temperature $\Delta T = 20$ °C centered at 30 °C. The line broadening due to temperature inhomogeneities in Ar is about ten times less than that in He, Ne, or N_2.

$$\nu = \nu(p,\overline{T}) + \delta T \left(\frac{\partial \nu}{\partial T}\right)_p, \tag{39}$$

where the rate of change of resonant frequency with temperature at a constant pressure is

$$\left(\frac{\partial \nu}{\partial T}\right)_p = \frac{p}{N_B k}\left(\frac{d}{dT}\right)\frac{\beta}{T} = -\frac{N}{N_B T}\left(\beta - \frac{T}{T_r}\frac{d\beta}{dx}\right). \tag{40}$$

Here T is the temperature in kelvins, $T-T_0$ is temperature in °C, and

$$x = \frac{T - T_0}{T_r} \tag{41}$$

is the parameter used by Bean and Lambert [23] for the convenient polynomial fits to their data. The characteristic temperature interval is $T_r = 1000$ K.

We can estimate the temperature spread ΔT needed to entirely account for the values of γ_2 measured in Ref. [10] by noting that for coherence that damps as $e^{-\gamma_2 t}$, the full width at half maximum $\Delta\nu$ of the Fourier transform is $\Delta\nu = \gamma_2/\pi$. Then

$$\gamma_2 = N\overline{v}\sigma_2 = \pi \left|\frac{\partial \nu}{\partial T}\right|_p \Delta T. \tag{42}$$

Solving Eq. (42) for ΔT with the values of σ_2 from Ref. [10] and with $|\partial\nu/\partial T|_p$ values that follow from Eq. (40) and the data of Ref. [23], we find that temperature spreads of only about 0.75 °C are sufficient to cause the large measured ^{85}Rb damping rates γ_2 in ^{4}He, Ne, and N_2 in Ref. [10]. In contrast, the measured γ_2 rate in Ar [10] is much lower, and is consistent with recent data [9]. We believe the Ar γ_2 data in Ref. [10] are not dominated by inhomogeneous

broadening, since a much larger temperature spread of 3.8 °C would be required.

IX. CONCLUSIONS

We have critically reviewed the literature on pressure shifts and damping rates of microwave transitions of alkali-metal atoms in buffer gases. For the buffer gas He we have developed a simple theory that is in good agreement with pressure shift measurements in Na, K, Rb, and Cs. The Carver rates reported in Ref. [10] for He and N_2 are more than a factor of 10 larger than those measured more recently [9] by a method that is independent of temperature gradients, and they are larger than the theoretical predictions of this paper by more than a factor of 20. However, there is good agreement between the two measurement methods for Ar, which is relatively insensitive to temperature gradients. The much smaller (compared to Ref. [10]) linewidths in N_2 that can be inferred from Carver rates reported in Ref. [9] have been confirmed in the recent experiments by Jau *et al.* [34]. This new evidence suggests that the homogeneous broadening of the microwave resonance lines of Rb vapor in He, Ne, and N_2 buffer gases is much smaller than that reported in Ref. [10] thirty years ago. A plausible reason for this discrepancy is a presence of small temperature gradients [11] that have led to inhomogeneous line broadening.

ACKNOWLEDGMENTS

We are grateful to A. Dalgarno, J. Vanier, T. Walker, D. Walter, E. Miron, and M. Romalis for discussions. This work was supported by AFOSR and DARPA.

[1] J. Vanier and C. Audoin, *The Quantum Physics of Atomic Frequency Standards* (Hilger, Philadelphia, 1989).
[2] W. E. Bell and A. L. Bloom, Phys. Rev. **107**, 1559 (1957).
[3] N. Cyr, M. Tetu, and M. Breton, IEEE Trans. Instrum. Meas. **42**, 640 (1993).
[4] J. Kitching, S. Knappe, and L. Hollberg, Appl. Phys. Lett. **81**, 553 (2002).
[5] P. L. Bender, E. C. Beaty, and A. R. Chi, Phys. Rev. Lett. **1**, 311 (1958).
[6] M. Arditi and T. R. Carver, Phys. Rev. **112**, 449 (1958).
[7] M. Arditi and T. R. Carver, Phys. Rev. **124**, 800 (1961).
[8] B. L. Bean and R. H. Lambert, Phys. Rev. A **12**, 1498 (1975).
[9] D. K. Walter, W. M. Griffith, and W. Happer, Phys. Rev. Lett. **88**, 093004 (2002).
[10] J. Vanier, J.-F. Simard, and J.-S. Boulanger, Phys. Rev. A **9**, 1031 (1974).
[11] J. Vanier kindly informed us that although great care was taken to avoid temperature gradients, it is still possible that the optical radiation incident on the cell may have caused such a gradient. However, its size is unknown.
[12] E. Fermi, Nuovo Cimento **11**, 157 (1934).
[13] T. F. O'Malley, Phys. Rev. **130**, 1020 (1963).
[14] U. Buck and H. Pauly, Z. Phys. **208**, 390 (1968).
[15] D. A. Varshalovich, A. N. Moskalev, and V. K. Khersonskii, *Quantum Theory of Angular Momentum* (World Scientific, Singapore, 1988).
[16] E. Clementi and C. Roetti, At. Data Nucl. Data Tables **14**, 177 (1974).
[17] J. Pascale, Phys. Rev. A **28**, 632 (1983).
[18] R. M. Herman, Phys. Rev. **137**, A1062 (1965).
[19] D. K. Walter, W. Happer, and T. G. Walker, Phys. Rev. A **58**, 3642 (1998).
[20] D. R. Bates and A. Damgaard, Philos. Trans. R. Soc. London, Ser. A **242**, 101 (1949).
[21] C. E. Moore, *Atomic Energy Levels*, Natl. Bur. Stand. (U.S.) Circ. No. 467 (U.S. GPO, Washington, D.C., 1952), Vol. II-III.
[22] E. Arimondo, M. Inguscio, and P. Violino, Rev. Mod. Phys. **49**, 31 (1977).
[23] B. L. Bean and R. H. Lambert, Phys. Rev. A **13**, 492 (1976).
[24] A. L. Bloom and J. B. Carr, Phys. Rev. **119**, 1946 (1960).
[25] A. T. Ramsey and L. W. Anderson, J. Chem. Phys. **43**, 191 (1965).
[26] E. C. Beaty, P. L. Bender, and A. R. Chi, Phys. Rev. **112**, 450 (1958).
[27] F. Strumia, N. Beverini, A. Moretti, and G. Rovera, Proc. Sympos. Freq. Control 30, 468 (1976).
[28] Y.-Y. Jau, N. N. Kuzma, and W. Happer, Phys. Rev. A **67**, 022720 (2003).
[29] M. A. Bouchiat and F. Grossêtete, J. Phys. (Paris) **27**, 353 (1966).
[30] B. S. Mathur, H. Y. Tang, and W. Happer, Phys. Rev. A **2**, 648 (1970).
[31] R. A. Bernheim, J. Chem. Phys. **36**, 135 (1962).
[32] S. Appelt, A. B.-A. Baranga, C. J. Erickson, M. V. Romalis, A. R. Young, and W. Happer, Phys. Rev. A **58**, 1412 (1998).
[33] A. B. A. Baranga, S. Appelt, M. V. Romalis, C. J. Erickson, A. R. Young, G. D. Cates, and W. Happer, Phys. Rev. Lett. **80**, 2801 (1998).
[34] Y.-Y. Jau, A. B. Post, N. N. Kuzma, A. M. Braun, M. V. Romalis, and W. Happer, Phys. Rev. Lett. **92**, 110801 (2004).